Chapter 1

The AlphaT Analysis

1.1 Analysis Overview

Events are binned in exclusive categories of H_T, and the multiplicity of jets and b-tagged jets, n_{jet} and n_{b}. Such binning allows for targetted interpretations across the vast array of possible simplified model final states, while reducing background yields to a minimum.

Analyses searching in the jets and $\not{E}_T$ final state encounter significant backgrounds from SM sources of both genuine $\not{E}_T$ [with associated jet production] and fake $\not{E}_T$, originating from jet mis-measurement. The α_{T} analysis makes predictions for the former using a data-driven transfer factor technique to extrapolate yields from statistically independent control samples into the signal region. However the latter, sources of fake $\not{E}_T$ from QCD multijet events, are reduced to a negligible level using the kinematic variable α_{T}.

The main analysis signal region is described in the remainder of this chapter, with background prediction techniques detailed later in chapter **??**.

1.1.1 The AlphaT kinematic variable

QCD multijet (MJ) events dominate the SM background in any search with multiple jets in the final state. Jet mis-measurements in a purely QCD MJ event can lead to non-negligible amounts of $\not{H}_T$, therefore passing the signal selection. Attempting to accurately measure this contribution is made very difficult given the hadronic environment of the LHC, and the lack of precise measurements and calculations of the large multijet cross sections. As an alternative approach, the goal of this analysis is to re-

duce QCD down to an entirely negligible level. This is achieved with the dimensionless kinematic variable, $\alpha_{\rm T}$ [REF]. This is defined for dijets as:

$$\alpha_{\rm T} = \frac{E_T^{j_2}}{M_T} \tag{1.1}$$

where $E_T^{j_2}$ is the transverse energy of the less energetic jet and M_T is the transverse mass of the dijet system, defined as:

$$M_T = \sqrt{\left(\sum_{i=1}^{2} E_T^{j_i}\right)^2 - \left(\sum_{i=1}^{2} p_x^{j_i}\right)^2 - \left(\sum_{i=1}^{2} p_y^{j_i}\right)^2} \tag{1.2}$$

where $E_T^{j_i}$, $p_x^{j_i}$ and $p_y^{j_i}$ are the transverse energy and transverse momentum in the x and y planes, for the jet j_i.

The $\alpha_{\rm T}$ variable can be generalised to an n-jet case by considering the event as a pseudo-dijet system, constructing each pseudo-jet such that the difference in H_T between each pseudo-jet system, ΔH_T, is minimised. $\alpha_{\rm T}$ then takes the form:

$$\alpha_{\rm T} = \frac{1}{2} \times \frac{H_T - \Delta H_T}{\sqrt{H_T^2 - \not{H}_T^2}} = \frac{1}{2} \times \frac{1 - \frac{\Delta H_T}{H_T}}{\sqrt{1 - \frac{\not{H}_T}{H_T}^2}} \tag{1.3}$$

A perfectly measured dijet event containing back to back jets in ϕ will have an $\alpha_{\rm T}$ value of 0.5, whereas events with $\not{H}_T$ originating from jet mis-measurements will have values of $\alpha_{\rm T} < 0.5$. Events containing sources of genuine $\not{E}_T$, whether from SM or BSM sources, have values of $\alpha_{\rm T} > 0.5$.

show plots of correlations between $\not{H}_T$ and ΔH_T for QCD, signal, SM real MET etc.

1.2 Hadronic Signal Region

This section outlines the relevant background sources of this analysis, and describes the basic hadronic pre-selection made for the signal region, as well as the relevant trigger requirements and data and simulation samples used.

1.2.1 SM Backgrounds

SM backgrounds are categorized into sources of genuine and fake missing energy.

Genuine EWK MET

Events containing leptonic decays of W bosons, $W \to \ell\nu$, originating either from direct W prodution, or via the decay of a top quark, are sources of genuine missing energy. The presence of a weakly interacting neutrino which evades detection leads to an energy imbalance. Such events are vetoed in the signal region due to the presence of a lepton, however if the lepton is missed for whatever reason, leptonic W decays can pass the signal selection, forming a significant SM background.

Leptons can be 'lost' for a variety different reasons, but ultimately for failing the lepton ID criteria. There are numerous potential causes, the most prevelant being soft-leptons below ID threshold or non-isolated leptons which pass the ID quality cuts but fail the isolation requirement.

SHOW TABLE WITH THE BACKGROUND BREAKDOWN - PUT INTO GRAPHICAL FORM?

Events containing a Single Isolated Track (SIT) are vetoed from the signal region. While originally designed to target hadronically decaying tau leptons, this requirement reduces the remaining lost-lepton backgrounds also.

The dominant EWK source of genuine missing energy comes from a Z-boson production where the Z decays via neutrinos, $Z \to \nu\bar{\nu}$, with associated jet production. This source of background is considered irreducible.

Following the reduction of such processes using the lepton, photon and SIT vetoes, any remaining contributions from SM EWK backgrounds are estimated using a fully data-driven transfer factor technique, described in detail in Section **??**.

Fake MET

As mentioned previously, the dominant source of background for analyses searching for a multijet final state is from QCD. A fully-measured QCD event would consist of multiple jets balancing each other in all planes, however in order to enter the signal region, an event must contain missing energy, $\not{H}_T$ (equivalent to $\not{E}_T$ in all-hadronic events).

The most common way for a balanced multijet (MJ) event to gain $\not{H}_T$ is when one or more of the jets are mis-measured, such that their vectorial sum then leads to non-zero $\not{H}_T$. This can due to badly calibrated or damaged segments of the calorimeter systems, or due to stochastic fluctuations within the jet-resolution of the detector. The former is protected against using a 'dead ECAL filter', where events are vetoed

if they contain significant energy deposits within a given distance from areas of the calorimeter system known to be either dead or damaged. The latter is dealt with using a cut on the α_{T} variable where events with fake missing energy signatures give values < 0.5.

QCD MJ events can also appear to contain non-zero missing energy due to the threshold requirements of jets. If an event contains one or more jets below the analysis threshold, then the event becomes imbalanced and will contain $\not{H}_T$. Events such as these are largely removed with the α_{T} requirement, however in addition a requirement is made on the ratio $\not{H}_T/\not{E}_T$.

1.2.2 Selection Criteria

The hadronic signal region requires at least 2 jets and that the topology has a value of α_{T} greater than 0.55. While no absolute $\not{E}_T$ requirement is made, the cut on α_{T} imposes an implied threshold, which maintains the analysis' sensitivity to very low regions of $\not{E}_T$. Events are also required to have at least $H_T > 200$GeV ensuring the presence of significant hadronic activity.

Any events containing leptons or photons are vetoed to ensure purely hadronic events are considered, thereby surpressing events with genuine $\not{E}_T$ from leptonic decays to neutrinos.

It is possible for events to acquire significant amounts of $\not{H}_T$ without having any real $\not{E}_T$ present when multiple jets are below the analysis threshold. To protect against this scenario, events are required to have a low ratio of the two variables, specifically $\not{H}_T/\not{E}_T < 1.25$.

Events can also acquire fake $\not{H}_T$ if they overlap with areas of the calorimater system which are damaged or known to be faulty, where jets can be mis-measured or lost as a result. To protect against this, for a given jet j, the angular seperation between the event $\not{H}_T$, calculated excluding jet j, and the jet itself is used, defined as:

$$\Delta\phi_j^* = \Delta\phi\Big(\overrightarrow{p_{\mathrm{T}j}}, -\sum_{i\neq j}\overrightarrow{p_{\mathrm{T}i}}\Big) \tag{1.4}$$

A small value of $\Delta\phi_j^*$ indicates that the momentum vector of j is aligned with the $\not{H}_T$ vector, implying the jet is mis-measured. Events are vetoed if a jet with $\Delta\phi^* < 0.5$ is within $\Delta R < 0.3$ of a known 'dead' region of the ECAL.

Following this preselection, events are further categorized into the three binning

dimenions of H_T, n_{b} and n_{jet}, as shown in table 1.1. Two jet multiplicity categories are defined as 2 or 3 jets, and 4 or more. B-tagged jet multiplicities are exactly 0, 1, 2, 3 or 4 and more. Combinations of these various categories are then further sub-divided into multiple H_T bins ranging from 200GeV up to an inclusive bin of $H_T > 1075$GeV.

Table 1.1 H_T binning used for each n_{jet} and n_{b} category.

(n_{jet},n_{b})	H_T bins (GeV)										
(2-3,0)	200–275	275–325	325–375	375–475	475–575	575–675	675–775	775–875	875–975	975–1075	>1075
(2-3,1)	200–275	275–325	325–375	375–475	475–575	575–675	675–775	775–875	875–975	975–1075	>1075
(2-3,2)	200–275	275–325	325–375	375–475	475–575	575–675	675–775	775–875	>875		
(≥4,0)	200–275	275–325	325–375	375–475	475–575	575–675	675–775	775–875	875–975	975–1075	>1075
(≥4,1)	200–275	275–325	325–375	375–475	475–575	575–675	675–775	775–875	875–975	975–1075	>1075
(≥4,2)	200–275	275–325	325–375	375–475	475–575	575–675	675–775	775–875	>875		
(≥4,3)	200–275	275–325	325–375	375–475	475–575	575–675	675–775	775–875	>875		
(≥4,≥4)	200–275	275–325	325–375	>375							

For bins of $H_T > 375$GeV the leading two jets in the event are required to have $p_{\mathrm{T}} > 100$GeV, with all additional jets having half the requirement of $p_{\mathrm{T}} > 50GeV$. In order to maintain a similar kinematic phase space throughout the many H_T bins, these jet p_{T} requirements are scaled for the lower H_T bins as shown in Table 1.2.

Table 1.2 Jet E_{T} thresholds per H_T bin.

H_T bin	200–275	275–325	325–375	>375
Lead jet	73.3	73.3	86.7	100.0
Second jet	73.3	73.3	86.7	100.0
All other jets	36.7	36.7	43.3	50.0

Example distributions are shown in figure 1.1, comparing data against MC.

1.2.3 Signal Triggers

Add emphasis on parked trigger, as it opens up phase space to compressed susy models

Events are collected at the HLT using a dedicated suite of signal triggers. For an event to pass the trigger requirements, it must exceed both a H_T and an α_{T} threshold. Trigger rate can be maintained by varying the threshold requirement on each of these independent 'legs', as shown in Table 1.3. Each H_T bin in the analysis is seeded by a single trigger, with a 25GeV offset in online and offline H_T, with the exception of the 200 GeV bin.

Trigger efficiencies are measured against an unbiased muon reference trigger, `HLT_IsoMu24_eta2p1`, using a muon tag and probe method where a single muon is selected and then subsequently ignored from the analysis when calculating event level variables such as H_T, $\not{H}_T$ and α_{T}. Efficiencies are measured for each H_T bin and

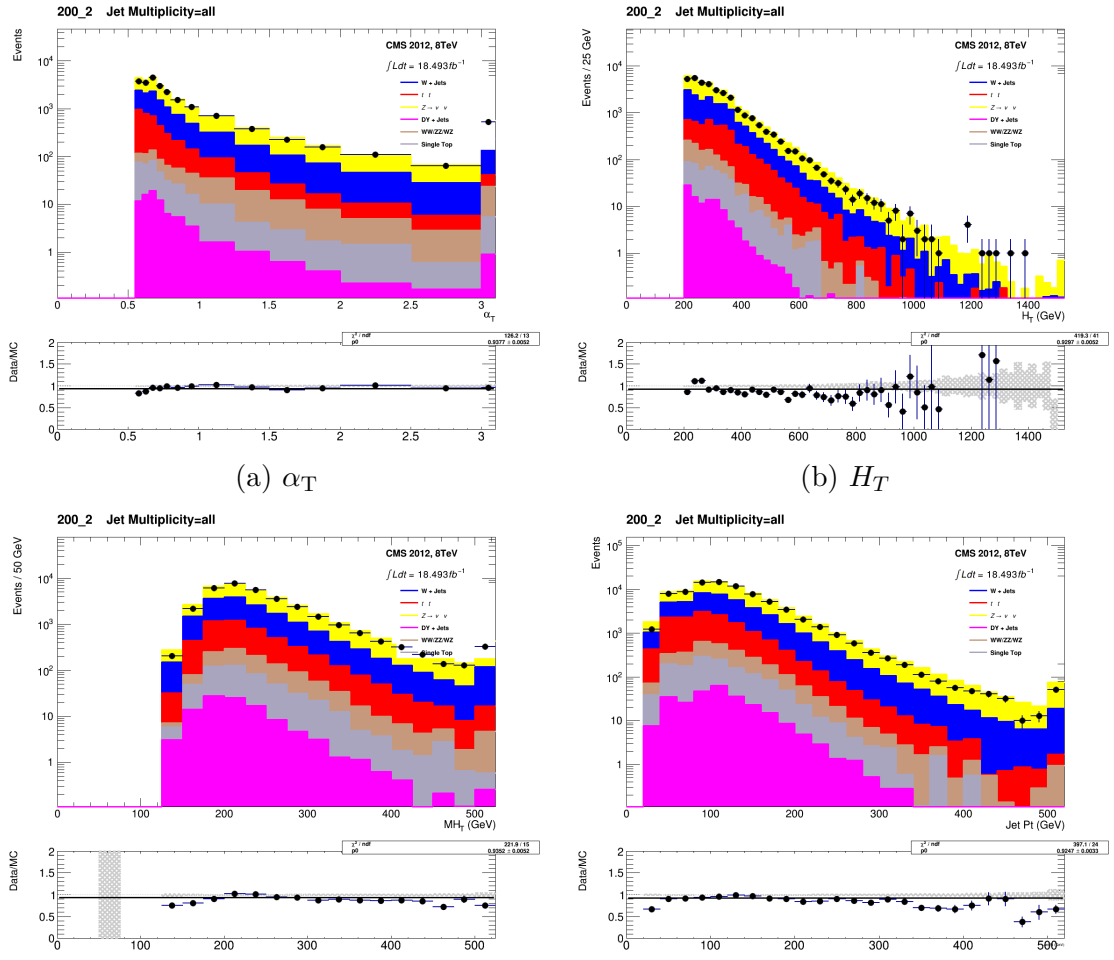

(a) α_{T} (b) H_T

(c) $\not{H}_T$ (d) Common Jet p_{T}

Fig. 1.1 Comparison of data with MC for the full hadronic signal selection. Plots are for $H_T > 200GeV, n_{\mathrm{jet}} \geq 2, n_{\mathrm{b}} \geq 0$.

Table 1.3 Signal triggers, the L1 seed triggers and their efficiencies measured for per H_T and n_{jet} category.

Offline H_T region (GeV)	Offline α_{T} threshold	L1 seed (L1_?) (highest thresholds)	Trigger (HLT_?)	Efficiency (%) $2 \leq n_{\mathrm{jet}} \leq 3$	Efficiency (%) $n_{\mathrm{jet}} \geq 4$
$200 < H_T < 275$	0.65	DoubleJetC64	HT200_AlphaT0p57	$81.8^{+0.4}_{-0.4}$	$78.9^{+0.3}_{-0.4}$
$275 < H_T < 325$	0.60	DoubleJetC64	HT200_AlphaT0p57	$95.2^{+0.3}_{-0.4}$	$90.0^{+1.2}_{-1.3}$
$325 < H_T < 375$	0.55	DoubleJetC64 OR HTT175	HT300_AlphaT0p53	$97.9^{+0.3}_{-0.3}$	$95.6^{+0.9}_{-1.0}$
$375 < H_T < 475$	0.55	DoubleJetC64 OR HTT175	HT350_AlphaT0p52	$99.2^{+0.2}_{-0.2}$	$98.7^{+0.5}_{-0.7}$
$H_T > 475$	0.55	DoubleJetC64 OR HTT175	HT400_AlphaT0p51	$99.8^{+0.1}_{-0.3}$	$99.6^{+0.3}_{-0.7}$

for each n_{jet} category, as summarised in table 1.3. Example trigger turn on curves are shown for the 3 lowest H_T bins in figures 1.2 and 1.3. Across the higher H_T bins the triggers are fully efficient, with some inefficiencies seen only in the lower H_T

bins. These innefficiencies are understood as being due to the L1 seed trigger used for this region, which had high thresholds in order to maintain low rates in the high PU environment throughout Run I. Lower efficiencies are also observed in the $n_{\text{jet}} \geq 4$ category attributed to the presence of softer jets, as an increased number of jets must equate to the same total H_T requirement of the bin.

All triggers were present throughout Run I, however the `HLT_HT200_AlphaT0p57` trigger was used as part of the 'Parked' stream of data which was reconstructed at a later date, following the active data-taking period. During data taking triggers may have 'prescale' factors applied to them such that only every n triggered events are actually recorded, however all of the signal triggers remained unprescaled for the entirety of the $8TeV$ data-taking.

1.2.4 Formula method

tie in with the split into nb and nj categories - necessary as stats will reduce, so we use this 'trick' to reduce errors

1.3 Datasets and MC samples

1.3.1 Datasets

The datasets used in this analysis are listed in Table 1.4. These include the primary signal sample datasets, named 'HTMHTParked', for which only Run2012A is absent as the parked trigger was present only during the run period's B, C and D. All other datasets contain events from triggers used for background estimation.

1.3.2 Montecarlo Background and Signal samples

The full list of montecarlo (MC) samples used in this analysis are listed in Table 1.5 along with the number of events, next-to-next-to-leading order (NNLO) cross section and an effective integrated luminosity for each.

can describe the different methods of MC generation

Each sample is weighted such that it's effective integrated luminosity is made equivalent to the relevant dataset luminosity. Event-by-event weights are applied such that the sample's PU distribution matches that as measured in data.

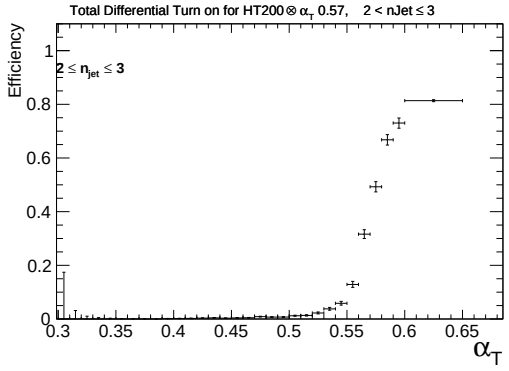

(a) Differential, $200 < H_T < 275$GeV

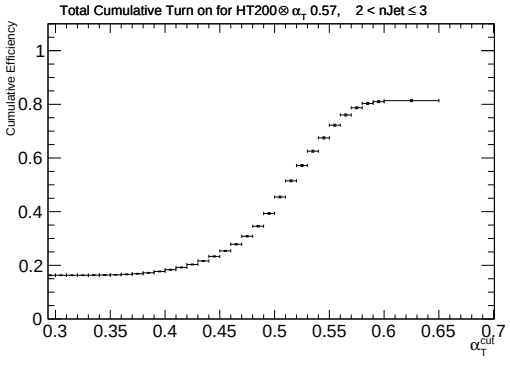

(b) Cumulative, $200 < H_T < 275$GeV

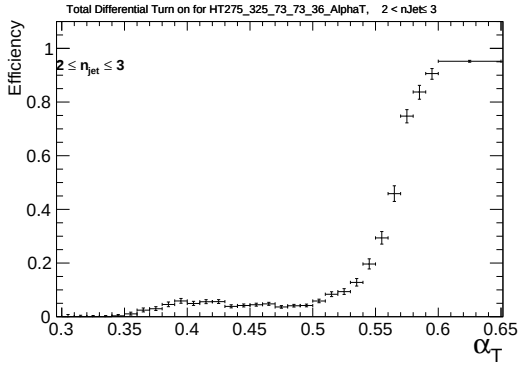

(c) Differential, $275 < H_T < 325$GeV

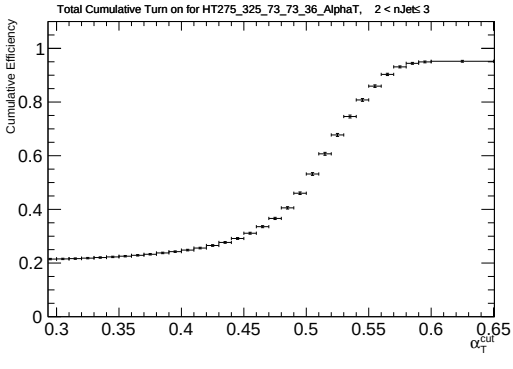

(d) Cumulative, $275 < H_T < 325$GeV

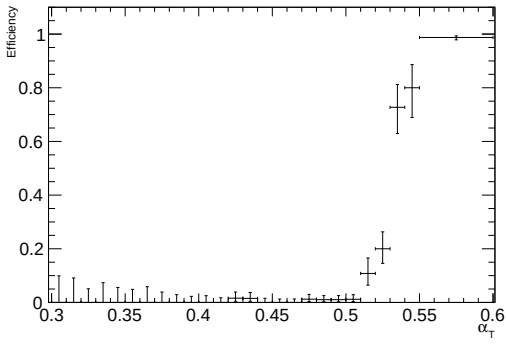

(e) Differential, $325 < H_T < 375$GeV

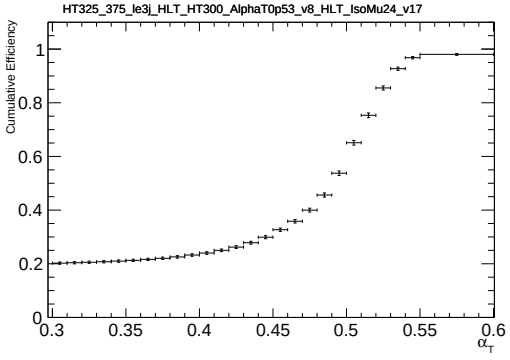

(f) Cumulative, $325 < H_T < 375$GeV

Fig. 1.2 *Maybe drop the differential turn-ons and just keep the cumu.* Differential (left) and Cumulative (right) efficiency turn-on curves for the signal triggers, for the three lowest H_T bins and $2 \leq n_{\text{jet}} \leq 3$.

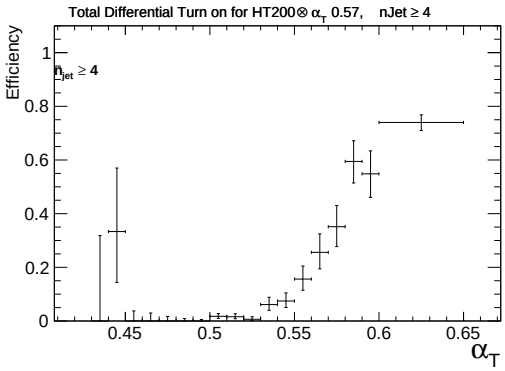

(a) Differential, $200 < H_T < 275$GeV

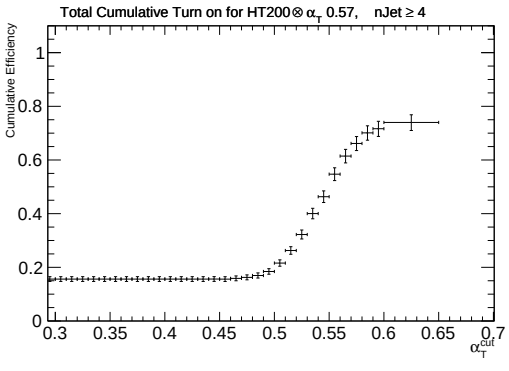

(b) Cumulative, $200 < H_T < 275$GeV

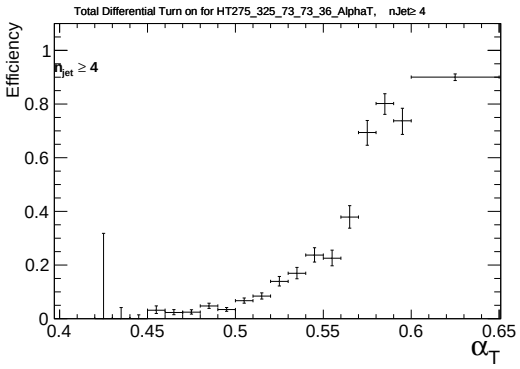

(c) Differential, $275 < H_T < 325$GeV

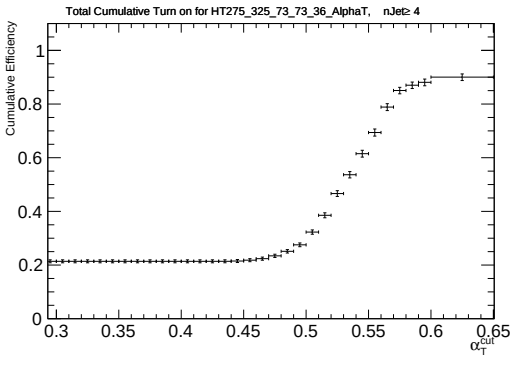

(d) Cumulative, $275 < H_T < 325$GeV

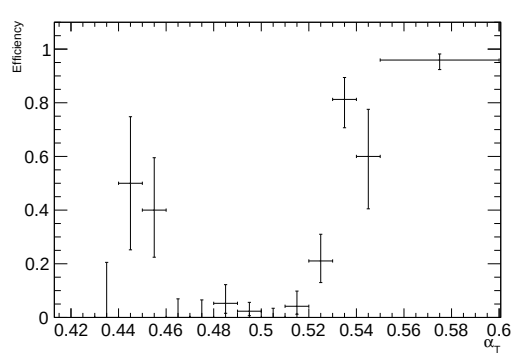

(e) Differential, $325 < H_T < 375$GeV

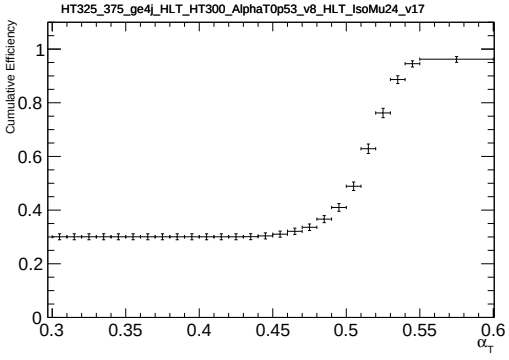

(f) Cumulative, $325 < H_T < 375$GeV

Fig. 1.3 *Maybe drop the differential turn-ons and just keep the cumu.* Differential (left) and Cumulative (right) efficiency turn-on curves for the signal triggers, for the three lowest H_T bins and $n_{\text{jet}} \geq 4$.

Table 1.4 $8TeV$ Datasets.

Dataset		Luminosity (fb^{-1})
/HTMHTParked/Run2012B-22Jan2013-v1/AOD		4.41
/HTMHTParked/Run2012C-22Jan2013-v1/AOD		6.80
/HTMHTParked/Run2012D-22Jan2013-v1/AOD		7.29
	Total	18.49
/HT/Run2012A-22Jan2013-v1/AOD		n/a
/JetHT/Run2012B-22Jan2013-v1/AOD		n/a
/JetHT/Run2012C-22Jan2013-v1/AOD		n/a
/JetHT/Run2012D-22Jan2013-v1/AOD		n/a
	Total	18.33
/SingleMu/Run2012A-22Jan2013-v1/AOD		0.69
/SingleMu/Run2012B-22Jan2013-v1/AOD		4.40
/SingleMu/Run2012C-22Jan2013-v1/AOD		6.77
/SingleMu/Run2012D-22Jan2013-v1/AOD		7.27
	Total	19.13
/Photon/Run2012A-22Jan2013-v1/AOD		0.68
/SinglePhoton/Run2012B-22Jan2013-v1/AOD		4.40
/SinglePhoton/Run2012C-22Jan2013-v1/AOD		6.77
/SinglePhotonParked/Run2012D-22Jan2013-v1/AOD		7.27
	Total	19.12

Table 1.5 MC samples for Standard Model processes.

Sample	N_{event}	Cross section (pb)	Corrected Cross section (pb)	Luminosity (fb^{-1})
/WJetsToLNu_TuneZ2Star_8TeV-madgraph-tarball/Summer12_DR53X-PU_S10_START53_V7A-v1/AODSIM	57661905	37509.0	34133.2	1.5
/WJetsToLNu_HT-150To200_8TeV-madgraph/Summer12_DR53X-PU_S10_START53_V7C-v1/AODSIM	21414209	253.8	234.53	84.4
/WJetsToLNu_HT-200To250_8TeV-madgraph/Summer12_DR53X-PU_S10_START53_V7C-v1/AODSIM	9895771	116.5	103.94	84.9
/WJetsToLNu_HT-250To300_8TeV-madgraph_v2/Summer12_DR53X-PU_S10_START53_V7A-v1/AODSIM	4924990	57.6	51.34	85.5
/WJetsToLNu_HT-300To400_8TeV-madgraph_v2/Summer12_DR53X-PU_S10_START53_V7A-v1/AODSIM	5141023	48.4	42.41	106.2
/WJetsToLNu_HT-400ToInf_8TeV-madgraph_v2/Summer12_DR53X-PU_S10_START53_V7A-v1/AODSIM	4923847	30.8	26.36	159.9
/ZJetsToNuNu_50_HT_100_TuneZ2Star_8TeV_madgraph(_ext)/Summer12_DR53X-PU_S10_START53_V7A-v1/AODSIM	23743998	452.8	405.21	52.4
/ZJetsToNuNu_100_HT_200_TuneZ2Star_8TeV_madgraph(_ext)/Summer12_DR53X-PU_S10_START53_V7A-v1/AODSIM	9876059	190.4	173.76	51.9
/ZJetsToNuNu_200_HT_400_TuneZ2Star_8TeV_madgraph(_ext)/Summer12_DR53X-PU_S10_START53_V7A-v1/AODSIM	9649619	45.1	42.41	214.0
/ZJetsToNuNu_400_HT_inf_TuneZ2Star_8TeV_madgraph(_ext)/Summer12_DR53X-PU_S10_START53_V7A-v1/AODSIM	5079710	6.26	5.81	811.5
/TT_CT10_TuneZ2star_8TeV-powheg-tauola/Summer12_DR53X-PU_S10_START53_V7A-v1(v2)/AODSIM	27094723	234.0	271.44	115.8
/TTZJets_8TeV-madgraph_v2/Summer12_DR53X-PU_S10_START53_V7A-v1/AODSIM	210160	0.172	0.172	1221.9
/T_t-channel_TuneZ2star_8TeV-powheg-tauola/Summer12_DR53X-PU_S10_START53_V7A-v1/AODSIM	3710227	56.4	56.4	65.8
/Tbar_t-channel_TuneZ2star_8TeV-powheg-tauola/Summer12_DR53X-PU_S10_START53_V7A-v1/AODSIM	1935072	30.7	30.7	63.0
/T_s-channel_TuneZ2star_8TeV-powheg-tauola/Summer12_DR53X-PU_S10_START53_V7A-v1/AODSIM	243961	3.79	3.79	64.4
/Tbar_s-channel_TuneZ2star_8TeV-powheg-tauola/Summer12_DR53X-PU_S10_START53_V7A-v1/AODSIM	139974	1.76	1.76	79.5
/T_tW-channel-DR_TuneZ2star_8TeV-powheg-tauola/Summer12_DR53X-PU_S10_START53_V7A-v1/AODSIM	497658	11.1	11.1	44.8
/Tbar_tW-channel-DR_TuneZ2star_8TeV-powheg-tauola/Summer12_DR53X-PU_S10_START53_V7A-v1/AODSIM	493460	11.1	11.1	44.5
/DYJetsToLL_M-10To50filter_8TeV-madgraph/Summer12_DR53X-PU_S10_START53_V7A-v1/AODSIM	7116223	13124.1	12205.4	0.5
/DYJetsToLL_M-50_TuneZ2Star_8TeV-madgraph-tarball/Summer12_DR53X-PU_S10_START53_V7A-v1/AODSIM	30171503	3503.7	3258.45	8.6
/DYJetsToLL_HT-200To400_TuneZ2Star_8TeV-madgraph(_ext)/Summer12_DR53X-PU_S10_START53_V7A-v1/AODSIM	6892777	24.3	22.24	283.7
/DYJetsToLL_HT-400ToInf_TuneZ2Star_8TeV-madgraph/Summer12_DR53X-PU_S10_START53_V7A-v1/AODSIM	2695789	3.36	3.11	802.3
/GJets_HT-200To400_8TeV-madgraph/Summer12_DR53X-PU_S10_START53_V7A-v1/AODSIM	57891147	1140.8	1060.9	50.7
/GJets_HT-400ToInf_8TeV-madgraph/Summer12_DR53X-PU_S10_START53_V7A-v1/AODSIM	9459562	124.7	115.97	75.9
/WW_TuneZ2star_8TeV_pythia6_tauola/Summer12_DR53X-PU_S10_START53_V7A-v1/AODSIM	9888431	57.1	57.1	173.2
/WZ_TuneZ2star_8TeV_pythia6_tauola/Summer12_DR53X-PU_S10_START53_V7A-v1/AODSIM	9841248	12.6	12.6	781.1
/ZZ_TuneZ2star_8TeV_pythia6_tauola/Summer12_DR53X-PU_S10_START53_V7A-v1/AODSIM	9751908	8.26	8.26	1180.6
/QCD_Pt-50to80_TuneZ2star_8TeV_pythia6/Summer12_DR53X-PU_S10_START53_V7A-v2	5950860	8148778	8148778 (LO)	0.001
/QCD_Pt-80to120_TuneZ2star_8TeV_pythia6/Summer12_DR53X-PU_S10_START53_V7A-v3	5962864	1033680	1033680 (LO)	0.006
/QCD_Pt-120to170_TuneZ2star_8TeV_pythia6/Summer12_DR53X-PU_S10_START53_V7A-v3	5985732	156293	156293 (LO)	0.038
/QCD_Pt-170to300_TuneZ2star_8TeV_pythia6/Summer12_DR53X-PU_S10_START53_V7A-v1(v2)	2015518O	34138	34138 (LO)	0.590
/QCD_Pt-300to470_TuneZ2star_8TeV_pythia6/Summer12_DR53X-PU_S10_START53_V7A-v1(v2,v3)	23588100	1759.5	1759.5 (LO)	13.4
/QCD_Pt-470to600_TuneZ2star_8TeV_pythia6/Summer12_DR53X-PU_S10_START53_V7A-v2	3978848	113.9	113.9 (LO)	34.9
/QCD_Pt-600to800_TuneZ2star_8TeV_pythia6/Summer12_DR53X-PU_S10_START53_V7A-v2	3964864	27.0	27.0 (LO)	146.8
/QCD_Pt-800to1000_TuneZ2star_8TeV_pythia6/Summer12_DR53X-PU_S10_START53_V7A-v2	3854563	3.55	3.55 (LO)	1085.8
/QCD_Pt-1000to1400_TuneZ2star_8TeV_pythia6/Summer12_DR53X-PU_S10_START53_V7A-v1	1964088	0.738	0.738 (LO)	2661.4
/QCD_Pt-1400to1800_TuneZ2star_8TeV_pythia6/Summer12_DR53X-PU_S10_START53_V7A-v1	1988062	0.0335	0.0335 (LO)	59345.1
/QCD_Pt-1800_TuneZ2star_8TeV_pythia6/Summer12_DR53X-PU_S10_START53_V7A-v1	977586	0.00183	0.00183 (LO)	534200

Interpretations are made using signal MC samples, each representing a scan in the phase space of a specific SMS model. The samples used are listed in Table 1.6. Each sample is generated at the parton level using MADGRAPH and then decayed using PYTHIA *(too vague?)*. Up to two additional partons are simulated in the initial generation step to ensure good modelling of initial state radiation (ISR), however supplementary samples were produced with up to three additional partons to allow for systematic studies into the effect on the analysis, as detailed in chapter **??**.

Table 1.6 MC samples for simplified models.

Model	Sample	Description
T2cc	/SMS-MadGraph_2J_T2cc_NoFilter_mStop-100to250_mLSP-20to230_8TeV-Pythia6Zstar/Summer12-START52_V9_FSIM-v1/AODSIM	Original scan
T2cc	/SMS-T2cc_NoFilter_mStop-175to250_mLSP-95to240_8TeV-Pythia6Z/Summer12-START52_V9_FSIM-v1/AODSIM	Original scan
T2cc	/SMS-T2cc_2J_mStop-250to350_mLSP-195to340_Tune22star_8TeV-madgraph-tauola/Summer12-START53_V19_FSIM-v2/AODSIM	Scan extension
T2cc	/SMS-8TeV_Pythia6Z_T2cc_3jets_mStop-200_mLSP-120/Summer12-START52_V9_FSIM-v1/AODSIM	3-parton sample
T2cc	/SMS-8TeV_Pythia6Z_T2cc_3jets_mStop-200_mLSP-190/Summer12-START52_V9_FSIM-v1/AODSIM	3-parton sample

1.3.3 Correcting SM sample cross sections

In order to increase statistics this analysis makes use of MC samples binned in parton-level H_T (H_T^{parton}). Leading order (LO) cross-sections are provided with these samples, which are translated into next-to-next-to-leading order (NNLO) cross-sections using translation-factors (k-factors) derived from corresponding inclusive samples. However, recent CMS studies (REF) have shown that the provided LO cross-sections for H_T^{parton} binned samples can be incorrect by up to 10%. This is shown in figure 1.4a, where un-physical steps are present in the ratio between the $\mathrm{Z}(\nu\nu)+\mathrm{jets}$ binned sample and the $\mathrm{DY}+\mathrm{jets}$ inclusive sample.

Two of the binned samples have corresponding inclusive samples to allow for this comparison to be made, namely $\mathrm{W}+\mathrm{jets}$ and $\mathrm{DY}+\mathrm{jets}$. For these two cases, the derivation of corrections for each H_T^{parton} binned sample is simple. However, for $\mathrm{Z}(\nu\nu)+$ jets and $\gamma+$ jets, no such inclusive samples exist. These binned samples are compared against the inclusive $\mathrm{DY}+$jets sample, where the overall normalisation is set according to the relative branching fraction of $Z \to \nu\bar{\nu}$ and GAMMA to $Z \to \ell\ell$, set as 0.505 and VALUE, respectively. An example ratio plot is shown in figure 1.4b, where a constant ratio between the samples is found.

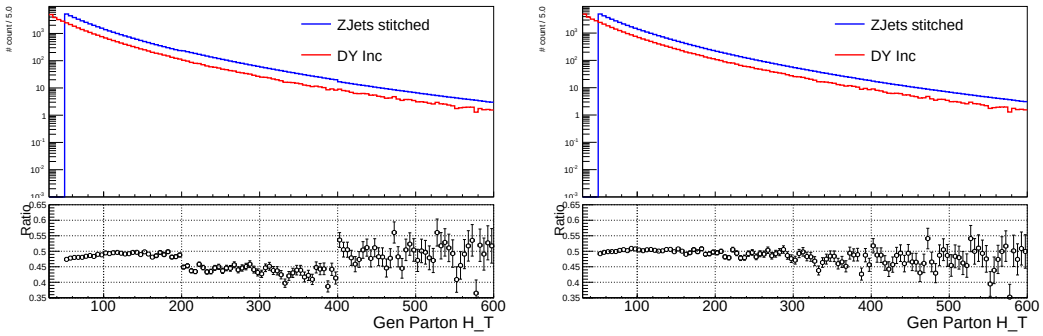

(a) No corrections. (b) With corrections.

Fig. 1.4 Generator-level H_T^{parton} distributions from the inclusive DY + jets and the H_T^{parton}-binned $\mathrm{Z}(\nu\nu)+\mathrm{jets}$ samples.

References